AN EXPERIMENTAL AND MODELING STUDY OF INGREDIANTS FOR PROPELLANT BURN-RATE ENHANCEMENT

M. P. Grams[a], W.R. Anderson, and R.C. Sausa*
U.S. Army Research Laboratory
Aberdeen Proving Ground, Maryland 21005-5069

ABSTRACT

Novel propellant formulations are critical for developing Future Force gun and missile systems that are safer, smaller, and more lethal than those used presently. We employ our US Army Research Laboratory combustion model, CYCLOPS, to predict the burning rates of nitrocellulose with and without HN_3, a stable pyrolysis product of high-nitrogen compound 5-aminotetrazole (5-AT). Our model employs a detailed chemical kinetic mechanism containing 368 chemical reactions and 59 species. We test its HN_3 chemistry by studying both neat and HN_3-doped flames experimentally and with the PREMIX flame code. We measure the major and radical species concentrations by either molecular beam mass spectrometry, laser spectroscopy, or both, and compare them to those we model with PREMIX using the detailed chemical mechanism. The model predicts well the concentration of the postflame species, including the OH concentration, which decreases by about 12 % with the addition of 1.1% HN_3. However, the model does not predict adequately the shapes of the HN_3 and NH profiles near the burner surface. Our rate and sensitivity analyses reveal that the rate expressions of reactions $HN_3+OH=N_3+H_2O$ and $HN_3+NH=NH_2+N_3$ should be lower by a factor of 3 and 4, respectively, than what is reported in the literature. Our CYCLOPS calculations with mechanism updates show that the addition of HN_3 to nitrocellulose enhances its burning rate significantly over the 10 to 300-MPa pressure range; a factor of approximately five at 10 MPa.

1. INTRODUCTION

The ability to either increase or decrease a propellant's burning rate by adding selective modifiers, without otherwise impairing its properties, is of great interest and a prerequisite for designing novel propellant formulations with tailored energy release. One use of interest is to achieve substantial burning rate differentials between otherwise similar, compatible propellant formulations for co-layered propellants in gun formulations (Leveritt et. al., 2006). Another is to achieve very high burning rates for rocket applications (Neidert, J., private communication). The high-nitrogen compound triamino-guanidinium azotetrazolate (TAGZT) is one example of a propellant modifier. It has the strongest burning rate augmentation effects known for HMX, RDX, and nitrate ester-based propellants (Flanagan, 1984; Walsh and Knott, 2004; Conner and Anderson, 2008). The action of this burning rate modifier may be associated with small, gas-phase intermediate species such as NH_3 and N_2H_4 that are produced in its decomposition. These species may be kinetically active by affecting the radical pool growth rate of the gas-phase flame thereby affecting the burning rate.

In this paper, we report the results of our two-phase, combustion model CYCLOPS for mixtures of nitrocellulose with HN_3. The model employs a detailed chemical kinetic mechanism that consists of over 350 reactions and nearly 60 species. We test key components of this mechanism for accuracy in the reaction's rate constants over a wide temperature range by performing both experimental and flame code modeling of neat and HN_3-doped flames. We measure the species concentrations by either molecular beam-mass spectrometry (MB/MS), laser-induced fluorescence (LIF), or both, throughout the flames, and compare them to those we predict with the PREMIX flame code employing the detailed chemical mechanism. Rate and sensitivity analysis reveal key species and chemical reactions important in the mechanism. We present these reactions and the burn-rate effects of HN_3 on nitrocellulose.

2. EXPERIMENTAL APPARATUS AND MODELING

Our previous publications contain the details of our burner apparatus, flame modeling, and CYCLOPS modeling (Grams and Sausa, 2008; Venizelos and Sausa, 2000; and Miller and Anderson, 2004). Briefly, our burner system is equipped for MB-MS, LIF, and thermocouple temperature measurements. A 60-mm flat burner (McKenna) mounted within a cylindrical, vacuum chamber supports the neat and HN_3-doped flames at 4 kPa. Vertical translation of the burner allows full optical access to the flame through the chamber view ports. We use gas flow rates of 0.86, 0.37, and 0.71 slm for H_2, O_2, and Ar, respectively, for the neat flame, and 0.86, 0.37, 0.69, and 0.02 for H_2, O_2, Ar, and HN_3, respectively, for the doped flame. The HN_3 flow rate corresponds to about

[a] *NRC/ARL Postdoctoral Research Associate*

Report Documentation Page

Form Approved
OMB No. 0704-0188

1. REPORT DATE	2. REPORT TYPE	3. DATES COVERED
DEC 2008	**N/A**	**-**

4. TITLE AND SUBTITLE	5a. CONTRACT NUMBER
An Experimental And Modeling Study Of Ingrediants For Propellant Burn-Rate Enhancement	5b. GRANT NUMBER
	5c. PROGRAM ELEMENT NUMBER
6. AUTHOR(S)	5d. PROJECT NUMBER
	5e. TASK NUMBER
	5f. WORK UNIT NUMBER
7. PERFORMING ORGANIZATION NAME(S) AND ADDRESS(ES) **U.S. Army Research Laboratory Aberdeen Proving Ground, Maryland 21005-5069**	8. PERFORMING ORGANIZATION REPORT NUMBER
9. SPONSORING/MONITORING AGENCY NAME(S) AND ADDRESS(ES)	10. SPONSOR/MONITOR'S ACRONYM(S)
	11. SPONSOR/MONITOR'S REPORT NUMBER(S)

12. DISTRIBUTION/AVAILABILITY STATEMENT
Approved for public release, distribution unlimited

13. SUPPLEMENTARY NOTES
See also ADM002187. Proceedings of the Army Science Conference (26th) Held in Orlando, Florida on 1-4 December 2008, The original document contains color images.

14. ABSTRACT

15. SUBJECT TERMS

16. SECURITY CLASSIFICATION OF:			17. LIMITATION OF ABSTRACT	18. NUMBER OF PAGES	19a. NAME OF RESPONSIBLE PERSON
a. REPORT	b. ABSTRACT	c. THIS PAGE			
unclassified	**unclassified**	**unclassified**	**SAR**	**6**	

1.1 % of the total flow rate. MKS mass flow controllers meter the gases, whose flow rates are cross-checked with a GCA wet test meter.

We model the flames with the PREMIX flame code (ver. 2.55) using the CHEMKIN mechanism interpreter (ver. 3.6) and chemical kinetics library (ver. 4.9) (Kee et al., 1985, 1991, 1994). Our calculations include both thermal diffusion and multitransport package options, and use either the measured temperature profile as input or solve the energy equation. The relevant reactions for HN_3 consumption and intermediate and final species' formation are from a literature review. We use the Sandia National Laboratories (SNL) Thermodynamic and Transport Databases for our calculations (Kee et al., 1985, 1985). The N_3 and HN_3 values, which are not included in the SNL Databases, are those of Burcat and Ruscic (Burcat and Ruscic, 2005).

The CYCLOPS model employs a detailed chemical mechanism containing 59 species and 368 chemical reactions. The bulk of this mechanism models successfully the burning rates of a propellant consisting mainly of nitrocellulose (Miller and Anderson, 2005). The present mechanism includes changes that pertain mainly to HN_3 decomposition reactions, and NH_x reactions or species. These modifications only modestly change our predicted burning rates for neat nitrocellulose.

Our propellant modeling relies on a pyrolysis law equation by Zenin and coworkers (Zenin et al., 1995). Its equation is as follows: $m\ (g) = m_o e^{Es/RT}$, where m (g) is the mass-flux, T is the surface temperature, R is the gas constant, $m_o = 1.8 \times 10^3$ g/cm^2 s, and E_s = 9935 cal/mole (Zenin, 1995; Miller and Anderson, 2005). We use the above equation for a given mass flux and a set of surface products (nascent gas phase products) to compute the heat feedback requirement to gasify the propellant; the code solves the corresponding gas-phase, flame problem and computes the heat feedback rate from the resulting flame structure (in particular, the near-surface properties, especially the temperature gradient in the gas phase at the surface). The code performs iterations on the mass flux, driven by an algorithm to cause the condensed heat flux requirement to converge to the gas heat flux supplied. When the problem converges, we easily relate the mass flux to the burning rate by means of the propellant density.

3. RESULTS AND DISCUSSION

Figure 1 shows the flame temperatures of both neat and HN_3-doped H_2/O_2/Ar flames measured with a thin-wire thermocouple, OH LIF, or both. The temperature at

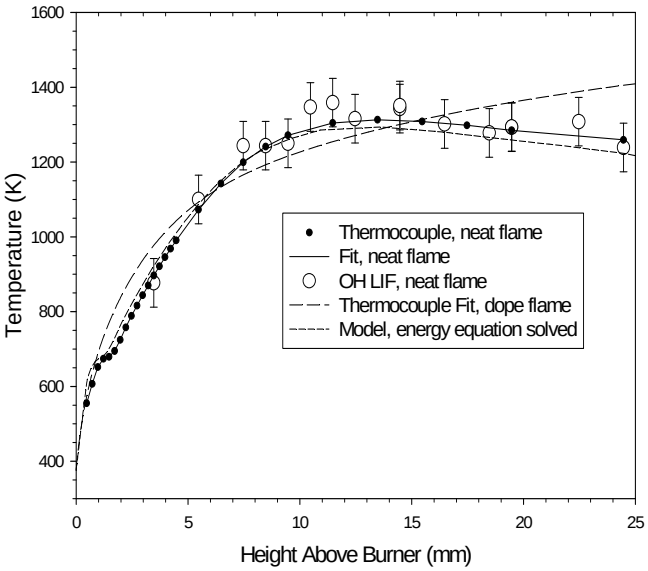

Fig. 1. Temperature profiles of an $H_2/O_2/HN_3$ flame

the burner surface is about 375 K for both flames. It increases from the burner surface to about 11 mm where it peaks at ~1300 K and then decreases gradually in the postflame region. When we add about 1% HN_3 to the neat flame, its temperature drops by about 50K at 15.0 mm. Figure 1 also shows the PREMIX temperature profile calculated by solving the energy equation. Overall, it is similar to the experimental profiles except in the postflame region. The calculated and experimental profiles diverge above 15 mm; the calculated one increases, whereas the experimental one gradually decreases. This divergence suggests that the model does not properly account for the gas-phase heat losses to the surroundings when solving the energy equation. Thus, our PREMIX calculations use the experimental temperature profiles as input for the species concentrations.

Figure 2 shows the experimental and calculated H_2, O_2, H_2O species profiles for the doped flame (~1% HN_3). The concentrations of H_2, O_2, and H_2O are similar to those in the neat flame as expected. Overall, the model profiles predict very well the experimental profiles throughout the flame. O_2 reacts completely with H_2 to form H_2O; however, H_2 does not react completely. Approximately one third of the initial H_2 is still present at 15 mm.

Figure 3 shows the experimental and modeled HN_3 profiles near the burner surface (3a, top), along with the

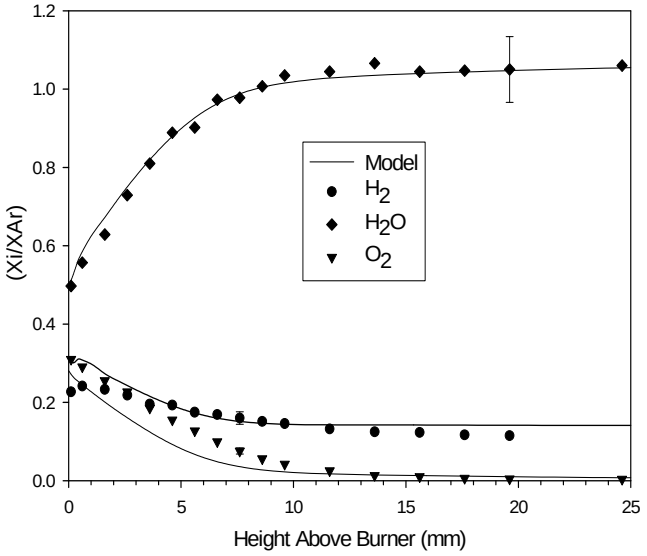

Fig. 2. Major species profiles of an $H_2/O_2/HN_3$ flame

results of our rate analysis (3b, bottom). As can bee seen in figure 3a, the model predicts HN_3 to react more rapidly than it does. Sensitivity analyses of the HN_3, NH, and NO species reveal that the rates of the following reactions $HN_3+OH=N_3+H_2O$ (R1) and $HN_3+NH=N_3+NH_2$ (R2) influence their concentrations, and that their rate expression should be lower than what is reported by LeBras and Combourieu and Li and coworkers (LeBras and Combourieu, 1973 and Li et al., 2006). When we lower these reaction's rate expressions by a factor of 4 and 3, respectively, in a modified mechanism, the model better predicts the experimental data, including our NH data (see Grams and Sausa, 2008). Our experimental data suggests that we could lower the rate expression of these reactions further; however, this would reduce the predicted NO concentration below our experimental uncertainty, as will be shown in the latter portion of this paper.

Figure 3b reveals that reactions $HN_3+OH=N_3+H_2O$, $HN_3+NH=N_3+NH_2$, and $HN_3+H=N_2+NH_2$ account for the disappearance of HN_3 close to the burner surface, where about 90% of HN_3 reacts with either OH or NH. The heat release of reaction $HN_3+OH=N_3+H2O$ is about 30% that of $H+O_2+M=HO_2+M$, the reaction with the largest heat release in this system (2.86 cal/cm3-sec).

Figure 4 shows both the N_2 experimental and calculated profiles for the HN_3-doped flame. Both models predict the N_2 concentration very well throughout the flame. The profiles show that the N_2 concentration gradually increases from the burner surface to about 7 mm, and then levels off in the postflame region. The model with the modified mechanism predicts an X_{N2}/X_{Ar}

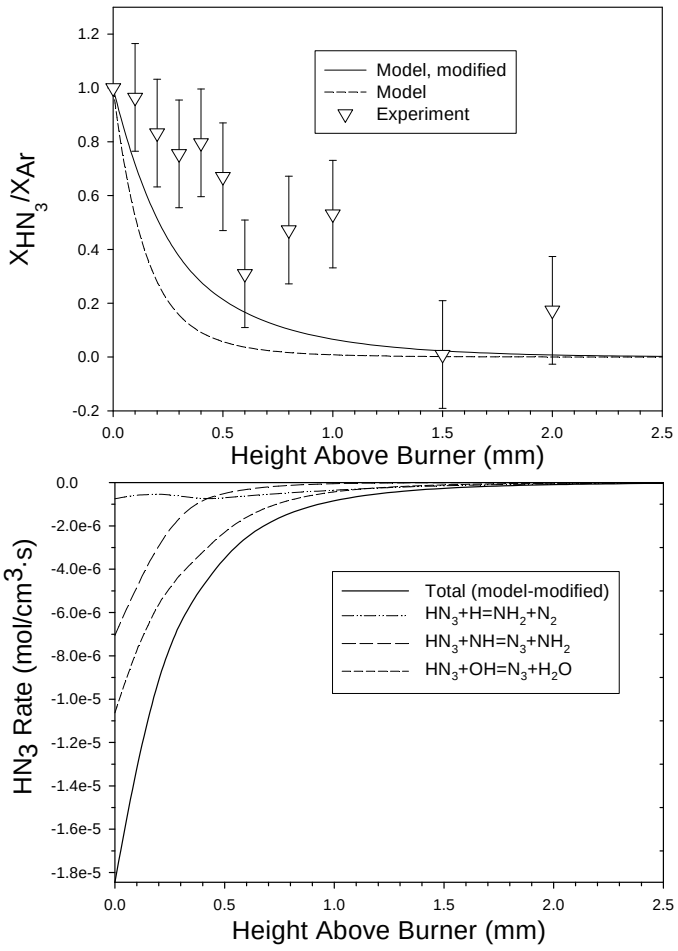

Fig. 3. HN_3 modeled and experimental profiles (top, 3a) with NH rate of production and consumption (bottom, 3b).

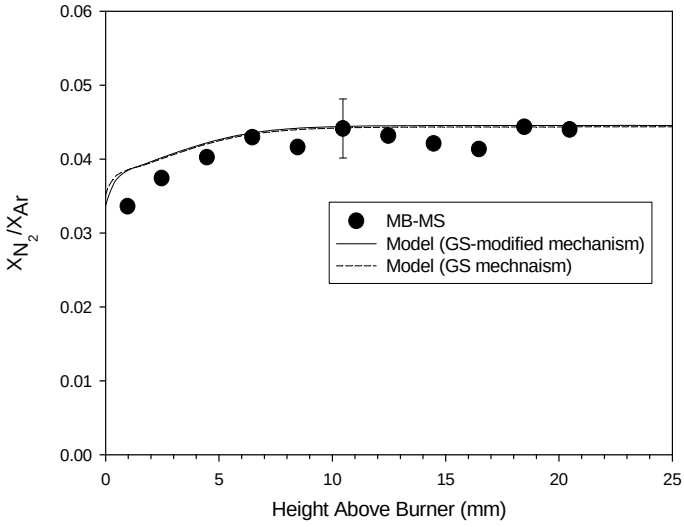

Fig. 4. N_2 modeled and experimental profiles

value of 0.0442 at 19.6 mm. This value is in excellent agreement with the experimental value of 0.044. A NASA-Glenn equilibrium calculation yields an X_{N2}/X_{Ar} value of 0.0452 at the adiabatic temperature, T=2543 K. These results show that the postflame N_2 concentration reaches its adiabatic equilibrium concentration at approximately 1300 K, and its concentration is mostly independent of temperature in the temperature range 1300 to 2500 K.

Presented in figure 5 are both the NO modeled and experimental profiles for the doped flame. The X_{NO}/X_{Ar} experimental value increases by about factor of two from burner surface to 7 mm, and then levels off mostly thereafter. The model with the modified mechanism predicts a value of 0.0038 near 13 mm. This value agrees well with the experimental value of 0.0042 at the same location, but not as well as the value from the original mechanism. We employ the modified mechanism, instead of the original mechanism because it predicts better the HN_3 experimental profile, as shown in figure 3a, and the NH profile, not shown (Grams and Sausa, 2008). Also, it predicts the NO postflame concentration fairly well, within the limits of our experimental uncertainty. A 5% increase in the inputted temperature profile, the uncertainty in our temperature measurement, decreases the X_{NO}/X_{Ar} value by about 2%, whereas a 5% decrease in the temperature profile increases the X_{NO}/X_{Ar} value by about 2%. These results reveal that the PREMIX postflame NO concentrations depend mostly on the chemical mechanism.

Figure 6 shows the OH experimental and modeled profiles for both the neat and HN_3-doped flames. The experimental profile of the neat flame is normalized to the modeled profile and serves as a basis for comparing the modeled OH concentrations to those determined experimentally in the doped flame. The modeled profiles are similar to the experimental profiles; the OH concentration decreases from the burner surface to about 3 mm, increases from 3 to 7-12 mm, and then decreases in the postflame region. The models predict well the overall shape of the experimental profiles, including their decay. However, the modeled profiles are shifted about 2 mm away from the burner compared to the experimental profiles. At present, this discrepancy is not well understood. Figure 6 reveals that the addition of ~1% HN_3 decreases the peak OH concentration by approximately 12%. This decrease is predicted very well by the model, which shows an 11.35% decrease in OH concentration.

Figure 7 shows the experimental burning rates of nitrocellulose and our predicted burning rates of nitrocellulose, and HN_3 and nitrocellulose, employing our modified mechanism in our calculations. Our model predicts very well the burning rates of nitrocellulose from

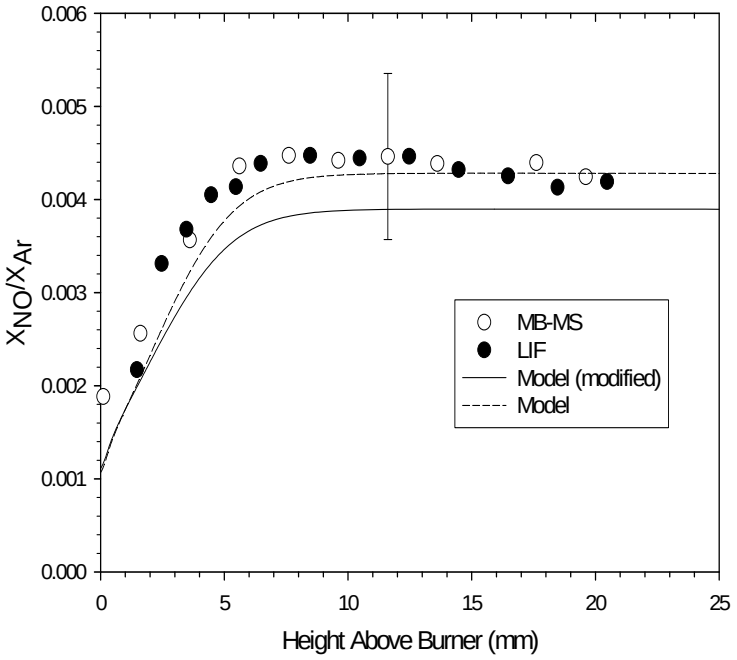

Fig. 5. NO Modeled and experimental profiles

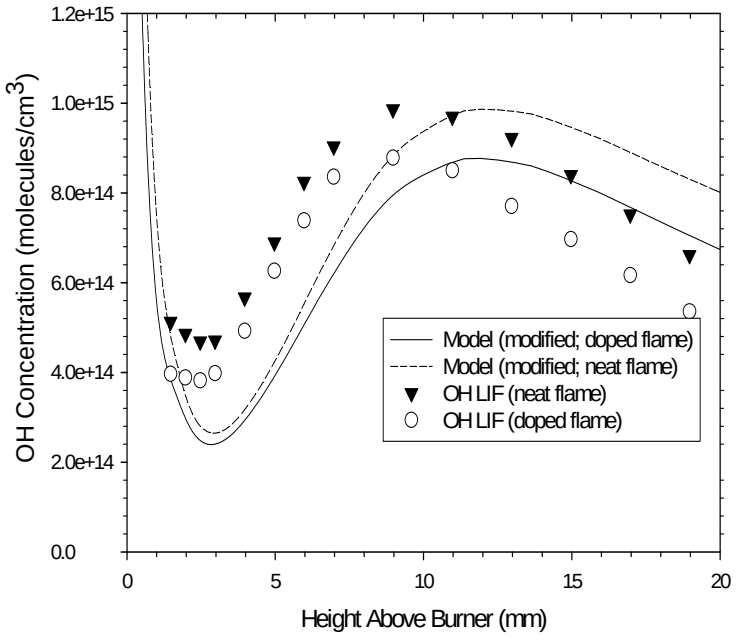

Fig. 6. Experimental and molded OH profiles in neat and HN_3 doped H_2/O_2 flame

about 0.5 to 350 MPa, and reveals that HN_3 strongly increases nitrocellulose's burning rate over the 1 to 200-MPa pressure range, as much as seven at 10 MPa. A detailed chemical analysis reveals that the following reactions play a prominent role in this augmentation process:

R3: $HN_3 \rightarrow NH + N_2$
R4: $NH + NO \rightarrow H + N_2O$
R5: $NN_3 + H \rightarrow N_3 + H_2$
R6: $HN_3 + OH \rightarrow N_3 + H_2O$
R7: $N_3 + NO \rightarrow N_2O + N_2$
R8: $N_2O + M \rightarrow N_2 + O + M$

HN_3 produces two effects leading to the increased burning rate: one, a more rapid conversion of NO to final product N_2, and two, some contribution from chain branching via the O-atom radical produced in R8 which speeds the kinetics. The relative proximity of the heat released by the NO conversion to the surface may be the primary reason for the very strong, burning rate augmentation. In fact, the NO conversion is predicted to become so fast that the dark zone that occurs for pure nitrocellulose at 10 atm due to NO formation collapses when HN_3 is added. That is, the first and second stage flames coalesce. The relative proximity of the heat released by the NO conversion to the surface as compared to NC, where the dark zone causes a large separation, may be the primary reason for the very strong burning rate augmentation effect.

CONCLUSION

The design of novel propellant formulations with tailored energy release is important for Future Force weapons systems. We have calculated the burning rates of nitrocellulose with and without HN_3 using our CYCLOPS combustion model with a detailed chemical kinetic mechanism composed of 368 chemical reactions and 59 species. We tested this mechanism's HN_3 chemistry by performing a combined experimental and modeling study of both neat and HN_3-doped H_2/O_2 flames. Our results show that the rates of reactions $HN_3+OH=N_3+H_2O$ and $HN_3+NH=NH_2+N_3$ should be lower by a factor of 3 and 4, respectively, than what is reported in the literature. Our CYCLOPS calculations with updated mechanism show that the addition of HN_3 to nitrocellulose increases its burning rate over a wide range of pressures used for rockets and guns.

ACKNOWLEDGMENTS

We thank Drs. C. Conner, R. Pesce-Rodriguez, and A. Kotlar of the US Army Research Laboratory for many helpful discussions, and the ARL Major Shared Resource Center (MSRC) for a grant of computer time

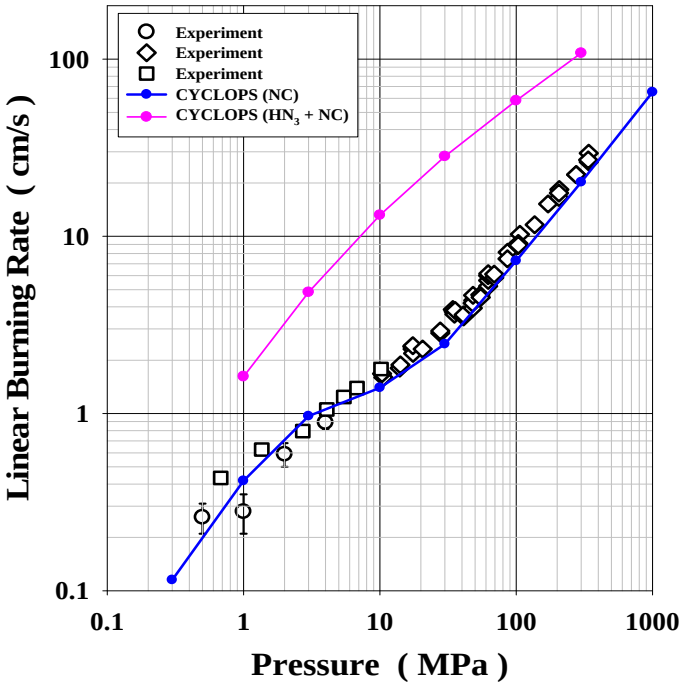

Fig. 7. Experimental and molded burning rates of nitrocellulose with and without HN_3

Research Council (MG) and the EQT Program (RCS and WRA) is gratefully acknowledged.

REFERENCES

Burcat, A. and Ruscic, B., 2005: Third Millennium Ideal Gas and Condensed Phase Thermochemical Database for Combustion with Updates from Active Thermochemical Tables, ANL-05/20 and TAE 960, Technion-IIT, Aerospace Engineering, and Argonne National Laboratory, Chemistry Division, September 2005.

Conner, C.B. and Anderson, W.R., 2008: Modeling the Combustion of JA2 and Solid Propellants of Similar Composition, Thirty-second Symposium (International) on Combustion, The Combustion Institute, Pittsburgh, PA, (2008), in press.

C.B. Conner, Chen, C.C. and W.R. Anderson, 2008: Chemical Kinetics of Solid Propellant Burning Rate Modifiers, 42nd JANNAF Combustion Subcommittee Meeting, Newton, MA, May, 2008

Flanagan, J.E., Frankel, M.B. and Woolery, D.O., 1994: HMX Combustion Modification, AFRPL TR-84-044, August 1984.

Grams, M.P. and Sausa, R.C., 2008: The Combustion of a Simple, High Nitrogen Compound: An Experimental and Modeling Study of a Low Pressure, Hydrazoic Acid-Doped Flame, 42nd JANNAF Combustion Subcommittee Meeting, Newton, MA, May, 2008

Kee, R.J., Grcar, J.F., Smooke, M.D. and Miller, J.A., 1985, 1991: A FORTRAN Program for Modeling Steady, Laminar, One-Dimensional Premixed Flames," Sandia national Laboratories Technical Report SAND 85-8240, December 1985; reprinted March 1991.

Kee, R.J., Rupley, F.M. and Miller, J.A., 1991: CHEMKIN-II: A FORTRAN Chemical Kinetics Package for the Analysis of Gas-Phase Chemical Kinetics. Sandia National Laboratories Report SAND89-8009, 1991; reprinted 1994.

Kee, R.J., Rupley, F.M. and Miller, J.A., 1987: The Chemkin Thermodynamic Data Base, Sandia National Laboratories Report SAND87-8215B (1987).

Kee, R.J., Dixon-Lewis, G., Warnatz, J., Coltrin, M.E. and Miller, J.A., 1986: A FORTRAN Computer Code Package for the Evaluation of Gas-Phase Multicomponent Transport Properties, Sandia National Laboratories Technical Report SAND86-8246 (1986).

LeBras G. and Combourieu, J., 1973: Reactions of atomic hydrogen and active nitrogen with hydrogen azide, *Int. J. Chem. Kinetics*, 5(4), 559-576.

Leveritt, C.S., Michienzi, C., Brant, A. and Knott, C., 2006: High-Energy Gun Propellants Containing High-Nitrogen Modifiers, Proceedings, 33rd JANNAF Propellant and Explosives Development and Characterization Subcommittee Meeting, Destin, Florida, March 2006, JSC CD-42.

Li, S., Zhang, Q. and Wang, W., 2006: *Ab initio* and variational transition state approach to atmospheric photooxidation: Mechanism and kinetics for the reaction of HN_3 with OH radical, *Chem. Phys. Let.*, 428(4-6), 262-267

Miller, M.S. and Anderson, W.R., 2004: Burning-rate predictor for multi-ingredient propellants: Nitrate-ester propellants, *Journal of Propulsion and Power*, 20(33), 440-454.

Miller, M.S. and Anderson, W.R., 2000: Energetic-Material Combustion Modeling with Elementary Gas-Phase Reactions: A Practical Approach, in: V. Yang, T.B. Brill, W.Z. Ren (Eds.), *Solid Propellant Combustion Chemistry, Combustion and Motor Interior Ballistics, Progress in Astronautics and Aeronautics*, Vol. 185, AIAA, Reston, VA, 501-531.

Miller, M.S., 2005: Burning-Rate Models and Their Successors, a Personal Perspective, in: *Overviews of Recent Research on Energetic Materials*, R.W. Shaw, T.B. Brill, and D.L. Thompson, Eds., Advanced Series in Physical Chemistry Vol. 16 (World Scientific, London, August 2005), chapter 13.

Venizelos, D.T. and Sausa, R.C., 2000: Detailed Chemical Kinetics Studies of an $NH_3/N_2O/Ar$ Flame by Laser-Induced Fluorescence, Mass Spectrometry, and Modeling, Proceedings of the Combustion Institute, Volume 28, 2411–2418.

Walsh, C. and Knott, C., 2004: High Nitrogen Burning Rate Modifiers for Gun Propellants, Proceedings, 32nd JANNAF Propellant Explosives Development and Characterization Subcommittee Meeting, Seattle, Washington, July 2004, JSC CD-34.

Zenin, A., 1995: HMX and RDX: Combustion Mechanism and Influence on Modern Double-Base Propellant Combustion, Journal of Propulsion and Power, 11(4), 752-758.